SCIENCE CHINA
Information Sciences

• RESEARCH PAPER •

September 2024, Vol. 67, Iss. 9, 192502:1–192502:15
https://doi.org/10.1007/s11432-023-4039-y

The quantum Ising model for perfect matching and solving it with variational quantum eigensolver

Qilin ZHENG[1], Pingyu ZHU[1], Chao WU[1], Miaomiao YU[1], Weihong LUO[1] & Ping XU[1,2*]

[1]*Institute for Quantum Information and State Key Laboratory of High Performance Computing, College of Computer Science and Technology, National University of Defense Technology, Changsha* 410073*, China;*
[2]*Hefei National Laboratory, Hefei* 230088*, China*

Received 21 December 2023/Revised 4 March 2024/Accepted 21 May 2024/Published online 19 August 2024

Abstract Obtaining all perfect matchings of a graph is a tough problem in graph theory, and its complexity belongs to the #P-Complete class. The problem is closely related to combinatorics, marriage matching problems, dense subgraphs, the Gaussian boson sampling, chemical molecular structures, and dimer physics. In this paper, we propose a quadratic unconstrained binary optimization formula of the perfect matching problem and translate it into the quantum Ising model. We can obtain all perfect matchings by mapping them to the ground state of the quantum Ising Hamiltonian and solving it with the variational quantum eigensolver. Adjusting the model's parameters can also achieve the maximum or minimum weighted perfect matching. The experimental results on a superconducting quantum computer of the Origin Quantum Computing Technology Company show that our model can encode 2^n dimensional optimization space with only $O(n)$ qubits consumption and achieve a high success probability of the ground state corresponding to all perfect matchings. In addition, the further simulation results show that the model can support a scale of more than 14 qubits, effectively resist the adverse effects of noise, and obtain a high success probability at a shallow variational depth. This method can be extended to other combinatorial optimization problems.

Keywords perfect matching, Ising model, quantum Hamiltonian, variational quantum eigensolver, quadratic unconstrained binary optimization

1 Introduction

The perfect matching number of a graph is an interesting problem in graph theory [1], which has a wide range of applications in Hall's marriage problem [2], the stable marriage problem [3], Kekulé structures [4], the Fries number of fullerenes [5], the monomer-dimer models [6], combinatorics [7], the Gaussian boson sampling [8], dense subgraphs [9], and the molecular vibration spectroscopy [10]. The number of perfect matchings can be given by calculating the Hafnian value of the corresponding adjacency matrix of the graph, and its complexity belongs to the #P-Complete class. The fastest algorithm with a time complexity of $O(n^3 2^{0.5n})$ for calculating Hafnian was proposed by Björklund in 2019 [11], and the Xanadu researchers designed the open-source Hafnian library [12] based on C++ and Python according to this algorithm. When the graph is bipartite, calculating the Hafnian of the adjacency matrix is equivalent to calculating its Permanent [13]. While Hafnian can give us the number of perfect matchings for a graph, it does not provide what the perfect matchings are for it. In the bipartite graph, if we need to obtain a specific perfect matching, we can use the Hungarian algorithm to solve it [14].

In addition to using classical computers to calculate the number of perfect matchings, Krenn et al. [1] discovered the link between perfect matchings and coherent superposition multi-particle states in 2017, and the method could use the coincidence counts of the optical quantum experimental device to give the Hafnian value, but they did not perform experimental verification. Brádler et al. [15] encoded the adjacency matrix of the graph into a Gaussian state and estimated the Hafnian value by measuring the probability of photons in each output mode, which was able to use the Gaussian boson sampling to

* Corresponding author (email: pingxu520@nju.edu.cn)

© Science China Press 2024

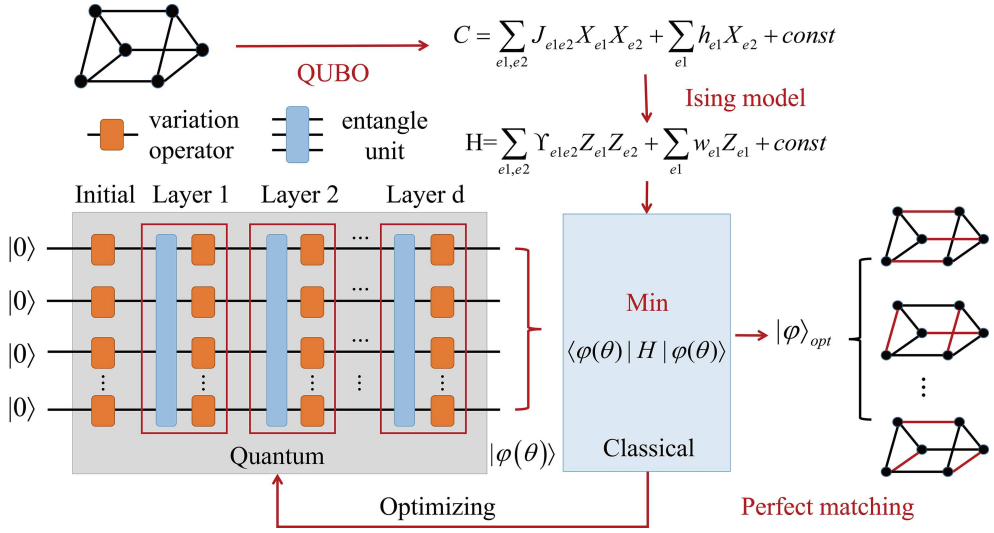

Figure 1 (Color online) Schematic diagram of the perfect matching model based on variation quantum computing.

complete the calculation of the Hafnian. Two years later, Wan et al. [16] completed the verification of this theory on a quantum chip. In 2023, Jianwei Pan's team enhanced two types of classical stochastic algorithms [17] for the Max-Haf problem [18] and Dense-k subgraph problem [8] by using the Gaussian boson sampling on "Jiu Zhang". These above methods used quantum properties for calculations, but none gave all specific perfect matchings.

In this paper, in order to solve all perfect matchings in the graph exactly. We propose a quadratic unconstrained binary optimization (QUBO) formula and map this formula to the quantum Ising Hamiltonian; then translate the perfect matchings into the ground state of the Hamiltonian. By performing eigenvalue decomposition on the Hamiltonian, we can obtain the number of perfect matchings and the specific perfect matching ground state according to the eigenvector corresponding to the smallest eigenvalue. On this basis, we use the variational quantum eigensolver (VQE) [19] to solve the ground state of the Hamiltonian, which can obtain all perfect matchings corresponding to the ground state of the graph.

The structure of the article is as follows, in Section 2, we propose a perfect matching QUBO formula and explain the specific mapping and solving process of perfect matchings to quantum Ising Hamiltonians. In Section 3, we simulate the problem by using the pyPanda [20] and the Qiskit [21] programming tools according to the proposed theory, and study the scalability of the model, the influence of variational depth on the model, and the behavior of the model under noise. In Section 4, we deploy the model to a superconducting quantum computer of the Origin Quantum Computing Technology Company [22] to experimentally verify the theory. In Section 5, we summarize the entire work.

2 Theory

For a random undirected graph $G=(V,E)$ that does not contain self-loops, where the number of nodes is $|V|=m$ and the number of edges is $|E|=n$. A single matching refers to the set of edges $E'\subset E$ where any two edges have no common node. When $|E'|=m/2$, it is a perfect matching. For an unweighted graph, our task is to find all perfect matchings with the number of edges equal to $m/2$. For a weighted graph, we need to find the maximum weighted perfect matching among them. The solution process includes the following steps, and Figure 1 shows the corresponding schematic diagram.

(1) Get the adjacency matrix or weighted adjacency matrix of the graph and name it A.

(2) Label the edges according to the upper triangular part of the matrix A. Each edge corresponds to a spin variable, and a total of n spin variables are required.

(3) Construct the QUBO formula for all perfect matchings according to the idea proposed by Lucas [23].

(4) Translate the QUBO formula into a quantum Ising Hamiltonian.

(5) Solve the ground state of the Ising Hamiltonian with the VQE. The ground state of the minimum energy corresponds to perfect matchings.

Algorithm 1 Spin labeling

Require: Vector $x[n]$; # The spin variable sequence
Matrix $A[m][m]$; # The adjacency matrix or weighted adjacency matrix
Ensure: Matrix $X[m][m]$;
Matrix $X[m][m] \leftarrow \emptyset$; # The spin matrix
Index $\leftarrow 1$;
for $u \leftarrow 0$ to $m-1$
  for $v \leftarrow 0$ to $m-1$
    If $v > u$ and $A[u][v]! = 0$
      $X[u][v] \leftarrow x$[index];
      index $\leftarrow$ index + 1;
    Else if $u = v$ or ($u < v$ and $A[u][v] = 0$)
      $X[u][v] \leftarrow \emptyset$;
    Else
      $X[u][v] \leftarrow X[v][u]$;
  End
End

2.1 Adjacency matrix

For an unweighted graph, its adjacency matrix A is defined as

$$A_{uv} = \begin{cases} 1, & \text{nodes } u \text{ and } v \text{ are connected,} \\ 0, & \text{nodes } u \text{ and } v \text{ are disconnected.} \end{cases} \tag{1}$$

For a weighted graph, let w_{uv} be the weight between nodes (u, v). The weighted adjacency matrix A is defined as

$$A_{uv} = \begin{cases} w_{uv}, & \text{nodes } u \text{ and } v \text{ are connected,} \\ 0, & \text{nodes } u \text{ and } v \text{ are disconnected.} \end{cases} \tag{2}$$

Therefore, the adjacency matrix or weighted adjacency matrix of a graph that does not contain a self-loop is a $m \times m$ dimensional symmetric square matrix with 0 on its diagonal.

2.2 Spin labeling

The edges are labeled according to the upper triangular part of the adjacency matrix, and each edge corresponds to a spin variable X_{uv} (or X_e), whose value is 0 or 1, and a total of n spin variables are required. Let the adjacency matrix of G be A, define the spin matrix X according to the process shown in Algorithm 1, and the numbering order is from left to right, then from top to bottom. The spin matrix is a symmetric matrix, except that there is a spin variable in the position where the adjacency matrix or weighted adjacency matrix is not 0, and there are no elements in other positions. For example, for $x = \{x_1, x_2, x_3, x_4\}$ and a adjacency matrix A, according to Algorithm 1, the corresponding spin matrix can be obtained as

$$A = \begin{bmatrix} 0 & 1 & 0 & 1 \\ 1 & 0 & 1 & 0 \\ 0 & 1 & 0 & 1 \\ 1 & 0 & 1 & 0 \end{bmatrix} \rightarrow X = \begin{bmatrix} & x_1 & & x_2 \\ x_1 & & x_3 & \\ & x_3 & & x_4 \\ x_2 & & x_4 & \end{bmatrix}. \tag{3}$$

2.3 Construct QUBO

Construct the QUBO formula that obtains all perfect matchings when it takes a minimum. Let $e1 = (u, v) \in E, e2 = (u2, v2) \in E$, where $u, u2, v, v2$ all belong to V. α_i is the adjustable parameter. The constraints that need to be met are as follows.

(1) Any two edges have no common vertices, so the number of edge conflicts is minimized. That is to say, the absolute value of the difference between the value summed for each row of the spin matrix X

and 1 is the smallest, and when it is the smallest, it means that there are no common vertices between all edges, specifically,

$$\begin{aligned} C_1 &= \alpha_1 \sum_{u\in V} \left(\sum_{\substack{v\in V,\\ (u,v)\in E}} X_{uv} - 1 \right)^2 \\ &= \alpha_1 \left(\sum_{u\in V} \sum_{\substack{e1\in E, e2\in E,\\ e1\cap e2=u, e1\neq e2}} X_{e1}X_{e2} - 2\sum_{e1\in E} X_{e1} + \sum_{u\in V} 1 \right). \end{aligned} \tag{4}$$

(2) The number of edges is equal to half of the number of nodes so that the number of edges meets the minimum energy when it is a perfect matching, specifically,

$$\begin{aligned} C_2 &= \alpha_2 \left(\frac{m}{2} - \sum_{\substack{(u,v)\in E,\\ v>u}} X_{uv} \right)^2 \\ &= \alpha_2 \left(\sum_{\substack{e1\in E, e2\in E,\\ e1\neq e2}} X_{e1}X_{e2} + (1-m)\sum_{e1\in E} X_{e1} + \frac{m^2}{4} \right). \end{aligned} \tag{5}$$

(3) Minimize the total weight of the edges participating in the matching, specifically,

$$C_3 = \alpha_3 \sum_{\substack{e1=(u,v)\in E,\\ v>u}} A_{uv}X_{e1}. \tag{6}$$

Therefore, the total QUBO formula is the sum of the above three items, namely $C = C_1 + C_2 + C_3$. Observe each item in C, and its highest order is $X_{e1}X_{e2}$. Without loss of generality, it can be abbreviated as $C = \sum_{e1,e2} J_{e1e2}X_{e1}X_{e2} + \sum_{e1} h_{e1}X_{e1} + \text{const}$.

2.4 Hamiltonian

Converting the QUBO formula into a quantum Ising Hamiltonian, the ground state corresponds to all perfect matchings, and the linear combination of the eigenvectors corresponding to its minimum eigenvalue is the perfect matching state. Let Z_e be the Pauli-Z matrix acting on the edge named e, namely $Z_e = \left[\begin{smallmatrix} 1 & 0 \\ 0 & -1 \end{smallmatrix}\right]$. Its eigenvalues are 1 and -1, and the corresponding eigenstates are $\mathrm{b}_1 = \left[\begin{smallmatrix} 1 \\ 0 \end{smallmatrix}\right]$ and $b_2 = \left[\begin{smallmatrix} 0 \\ 1 \end{smallmatrix}\right]$. For the basis $b \in \{0,1\}^n$ and $X_e \in \{0,1\}$, we have

$$Z_e \left|b\right\rangle = (-1)^{X_e} \left|b\right\rangle = (1-2X_e) \left|b\right\rangle \Rightarrow X_e \left|b\right\rangle = \frac{1-Z_e}{2} \left|b\right\rangle. \tag{7}$$

Therefore, each binary variable X_e can be substituted by $(1-Z_e)/2$. In addition, when X_e is a binary variable, $X_e = {X_e}^2$. Continuously applying the above two substitution rules, all C_i in the QUBO formula can be replaced by the quantum Ising formula composed of Pauli-Z operator, specifically,

(1) Calculating H_1 according to C_1,

$$\begin{aligned} C_1=&\alpha_1\sum_{u\in V}\left(\sum_{\substack{v\in V,\\(u,v)\in E}}X_{uv}-1\right)^2\\ \Rightarrow H_1=&\alpha_1\left(\sum_{u\in V}\sum_{\substack{e1\in E,e2\in E,\\e1\cap e2=u,e1\neq e2}}\frac{1-Z_{e1}}{2}\times\frac{1-Z_{e2}}{2}-2\sum_{e1\in E}\frac{1-Z_{e1}}{2}+\sum_{u\in V}1\right)\\ =&\alpha_1\begin{pmatrix}\frac{1}{4}\sum\limits_{u\in V}\sum\limits_{\substack{e1\in E,e2\in E,\\e1\cap e2=u,e1\neq e2}}Z_{e1}Z_{e2}\\ -\frac{1}{4}\sum\limits_{u\in V}\sum\limits_{\substack{e1\in E,e2\in E,\\e1\cap e2=u,e1\neq e2}}(Z_{e1}+Z_{e2})+\sum\limits_{e1\in E}Z_{e1}\\ +\frac{1}{4}\sum\limits_{u\in V}\sum\limits_{\substack{e1\in E,e2\in E,\\e1\neq e2,e1\cap e2=u}}1-n+m\end{pmatrix}. \end{aligned} \tag{8}$$

(2) Calculating H_2 according to C_2,

$$\begin{aligned} C_2=&\alpha_2\left(\frac{m}{2}-\sum_{\substack{e=(u,v)\in E,\\u<v}}X_{uv}\right)^2\\ \Rightarrow H_2=&\alpha_2\left(\sum_{\substack{e1\in E,e2\in E,\\e1\neq e2}}\frac{1-Z_{e1}}{2}\times\frac{1-Z_{e2}}{2}+(1-m)\sum_{e1\in E}\frac{1-Z_{e1}}{2}+\frac{m^2}{4}\right)\\ =&\alpha_2\begin{pmatrix}\frac{1}{4}\sum\limits_{\substack{e1\in E,e2\in E,\\e1\neq e2}}Z_{e1}Z_{e2}\\ -\frac{1}{4}\sum\limits_{\substack{e1\in E,e2\in E,\\e1\neq e2}}(Z_{e1}+Z_{e2})+\frac{m-1}{2}\sum\limits_{e1\in E}Z_{e1}\\ +\frac{1}{4}\sum\limits_{\substack{e1\in E,e2\in E,\\e1\neq e2}}1+\frac{1}{2}n(1-m)+\frac{m^2}{4}\end{pmatrix}. \end{aligned} \tag{9}$$

(3) Calculating H_3 according to C_3,

$$\begin{aligned} C_3=&\alpha_3\sum_{\substack{e1=(u,v)\in E,\\v>u}}A_{uv}X_{uv}\Rightarrow H_3=\alpha_3\sum_{\substack{e1=(u,v)\in E,\\v>u}}A_{uv}\frac{1-Z_{e1}}{2}\\ =&\alpha_3\begin{pmatrix}-\frac{1}{2}\sum\limits_{\substack{e1=(u,v)\in E,\\v>u}}A_{uv}Z_{e1}+\\ \frac{1}{2}\sum\limits_{\substack{e1=(u,v)\in E,\\v>u}}A_{uv}.\end{pmatrix}. \end{aligned} \tag{10}$$

Sum all of the above sub-Hamiltonians H_i; then the total Hamiltonian is

$$H=H_1+H_2+H_3. \tag{11}$$

Observe each term in the Hamiltonian H, and it includes the coupling term $Z_{e_1}Z_{e_2}$, the weighted term Z_{e_i}, and the constant term. Since constant terms do not affect the optimization process, they can be ignored here. Without losing generality, the Hamiltonian can be written as $H=\sum_{e1,e2}\gamma_{e1e2}Z_{e1}Z_{e2}+\sum_{e1}w_{e1}Z_{e1}$. When $\alpha_1=1,\alpha_2=1,\alpha_3=0$, the ground state of the minimum energy corresponds to all perfect matchings. When $\alpha_1=1,\alpha_2=1,\alpha_3=-1$, the ground state corresponds to a perfect matching with the maximum weight. When $\alpha_1=1,\alpha_2=1,\alpha_3=1$, the ground state corresponds to a perfect matching with the least weight.

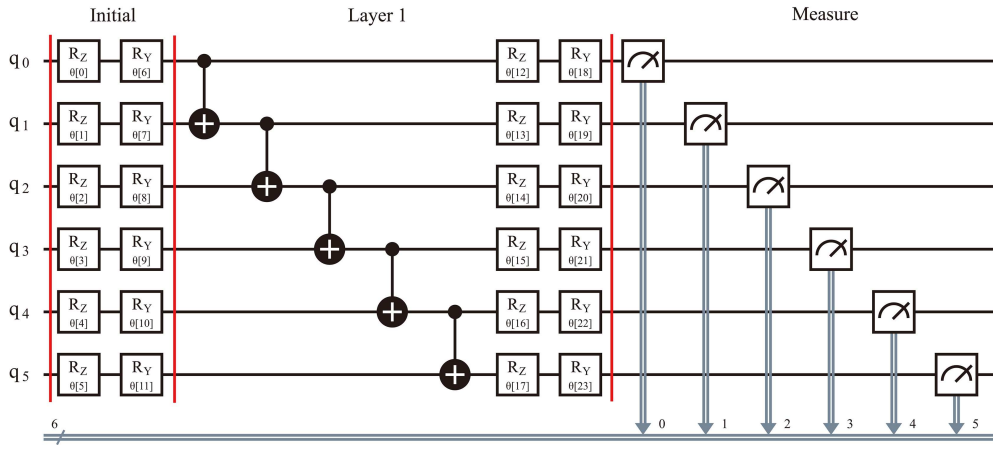

Figure 2 (Color online) Quantum circuit diagram of 6 qubits with a variational depth of 1 layer including the initial, variational, and measurement layers.

2.5 Finding the ground state

After constructing the total Hamiltonian H of the problem, the variational eigenvalue solver can be used to find the ground state of the quantum Ising Hamiltonian, and the linear combination of the eigenstates corresponding to the minimum energy value is perfect matchings. When the global constant is ignored, since all observations of the Hamiltonian H consist only of the coupling term $Z_{e_1}Z_{e_2}$ and the weighted term Z_{e_i}, both of which are diagonal operators, the total operator H summed for each is also diagonal. Let $H|\phi_i\rangle = \lambda_i|\phi_i\rangle$, that is, ϕ_i is the eigenvector corresponding to λ_i. Considering the degeneracy case, let $\lambda_{\min}$ be the smallest value of all eigenvalues, and its corresponding indexes form the set M, and the number of elements in M is equal to the number of perfect matchings; then all eigenvectors corresponding to the eigenvalue can be expressed as $|\phi_i\rangle_{i\in M}$. According to [19], the eigenvalue problem of observable values represented by the operator H can be reformulated as the variational problem on the Rayleigh-Ritz quotient, such that the linear combination $\sum_{i\in M}\beta_i|\phi_i\rangle$ of all eigenvectors corresponding to the smallest eigenvalue is the optimal solution $|\varphi(\theta^*)\rangle$ that minimizes $\langle\varphi(\theta)|H|\varphi(\theta)\rangle$, of which $\sum_{i\in M}|\beta_i|^2 = 1$. The variational operator consists of two parts, the first part is the variational initialization operator of the state, and the second part is the variational operator composed of the alternating combination of the entanglement operator and variational unit. The variational operator considered in this paper is composed of $R_Z(\theta) = \left[\begin{smallmatrix} e^{-i\theta/2} & 0 \\ 0 & e^{i\theta/2} \end{smallmatrix}\right]$ and $R_Y(\theta) = \left[\begin{smallmatrix} \cos(\theta/2) & -\sin(\theta/2) \\ \sin(\theta/2) & \cos(\theta/2) \end{smallmatrix}\right]$. Specifically, for the variational operator with depth d,

$$\begin{aligned} |\varphi(\theta)\rangle &= U_{\mathrm{VQC}}|0\rangle \\ &= [U_{\mathrm{single}}(\theta)U_{\mathrm{entangle}}]^d U_{\mathrm{single}}(\theta)|0\rangle \\ &= \left[\begin{array}{l} \left(\bigotimes_{i=0}^{n-1} R_Y(i,\theta_{2\mathrm{nd}+n+i}) \times \bigotimes_{i=0}^{n-1} R_Z(i,\theta_{2\mathrm{nd}+i})\right) \\ \times \left(\prod_{i=0}^{n-2} CX(i,i+1)\right) \end{array}\right]^d \\ &\quad \times \left(\bigotimes_{i=0}^{n-1} R_Y(i,\theta_{n+i}) \times \bigotimes_{i=0}^{n-1} R_Z(i,\theta_i)\right)|0\rangle. \end{aligned} \tag{12}$$

This variational circuit can generate arbitrary n-bit binary strings, which includes the entire optimization space of the perfect matchings. Figure 2 shows a variational circuit of 6 qubits with a depth $d = 1$. After constructing the experimental wave function, we can use the classical optimizer to minimize the

expected value,

$$\begin{aligned}\langle\varphi(\theta)|H|\varphi(\theta)\rangle &= \langle\varphi(\theta)|\sum_{e1,e2}\gamma_{e1e2}Z_{e1}Z_{e2}|\varphi(\theta)\rangle + \langle\varphi(\theta)|\sum_{e1}w_{e1}Z_{e1}|\varphi(\theta)\rangle \\ &= \sum_{e1,e2}\gamma_{e1e2}\langle\varphi(\theta)|Z_{e1}Z_{e2}|\varphi(\theta)\rangle + \sum_{e1}w_{e1}\langle\varphi(\theta)|Z_{e1}|\varphi(\theta)\rangle \\ &= \sum_{i}\lambda_i|\langle\phi_i|\varphi(\theta)\rangle|^2.\end{aligned} \tag{13}$$

Unless otherwise specified, the optimization tool used in this study is the COBYLA optimizer [24, 25]. Preparing $|\varphi(\theta)\rangle$ by changing the variational parameters, and minimizing the expected value $\sum_i \lambda_i|\langle\phi_i|\varphi(\theta)\rangle|^2$, we can prepare a linear combination of eigenvectors corresponding to all perfect matchings, that is $\sum_{i\in M}\beta_i|\phi_i\rangle$. When it converges to the theoretical minimum, the algorithm ends, and the experiment with the lowest energy value stores the optimal parameter θ^* for reconstructing the linear combination of eigenvectors and the linear combination of the eigenvectors output by the circuit is the encoding of the answer. Repeating the above optimization process, configuring each set of optimal parameters θ^* into the original variational circuit for sampling, we can get the distribution $D = |\langle\phi_i|\varphi(\theta^*)\rangle|^2 = |\beta_i|^2$. Considering the equivalence of each perfect matching, the expectation value for the probability of each perfect matching after sampling under the optimal parameters of multiple random initializations and optimization is $|\beta_i|^2 = \frac{1}{|M|}$, this can also be used as a basis for judging the number of perfect matchings and what each perfect matching is. One advantage of using this sampling method over adiabatic methods is that the target quantum Ising Hamiltonian can be computed directly, making the model independent of device connectivity.

3 Model simulation

3.1 Scalability of the model

In order to study the scalability of the model, we select the Cycle graph of $m \geqslant 6$ with even-numbered nodes for testing. A Cycle graph with m nodes has m edges, the degree of each node is 2, and the number of perfect matchings for each Cycle graph is 2. We select the number of variational circuit layers in the experiment as $d = 1$, and the variational parameters are initialized as an equal-weight superposition state. That is, the probability of all items in the quantum state is $1/2^m$. Specifically, let all parameters of R_Y be $\pi/2$ for the initialization operator and all other parameters θ in the variational operator be 0. Taking the 6-qubits circuit diagram shown in Figure 2 as an example, the initial configuration of the equal weight superposition state is to make $\theta_{[6]}$ to $\theta_{[11]}$ be $\pi/2$, and the rest of the parameters are 0. All the quantum states generated under this circuit configuration have a probability of $1/2^6$. We use pyPanda to simulate the problem, and the scale is selected as $[6, 8, 10, 12, 14]$, and the corresponding graphs and their perfect matchings are shown in Figure 3(a). Each optimization repeats ten times, and each experiment samples 8196 times. Figure 3(b) shows the experimental results, where costs are the mean values of $\langle\varphi(\theta)|H|\varphi(\theta)\rangle$, and success probabilities are the sum of probability of all perfect matching items. It can be seen that as the number of iterations increases, the costs gradually decrease and converge to their respective theoretical values, and the success probability continues to increase and converge. This shows that the optimization process plays a role in the proposed model. Table 1 shows more detailed results, where Params is the number of variational parameters in the circuit, Cost_theo represents the theoretical loss function value, and Cost_sim is the loss function value under each optimal parameter, Suc_prob is the success probability of sampling under the optimal parameters of each optimization, that is, the sum of the probabilities of all perfect matching items. For problems of different scales, our model can obtain the ground state corresponding to the perfect matching with a high success probability. For Cycle graph 14, the minimum eigenvalue of Hamiltonian after the eigenvalue decomposition is -10.5, 10 optimizations converge to 5462 (1010101010110) and 10921 (10101010101001), and the success probability of these two perfect matchings is 0.989 ± 0.011, which shows that the simulation scale can reach more than 14 qubits. In order to verify the performance of the proposed model on other types of graphs, as shown in the upper part of Figure 3(c), we randomly generated three groups of 14-edge graphs, which contained 6, 8, and 10 nodes, respectively. The bottom parts of Figure 3(c) show the results of the optimization. We can see

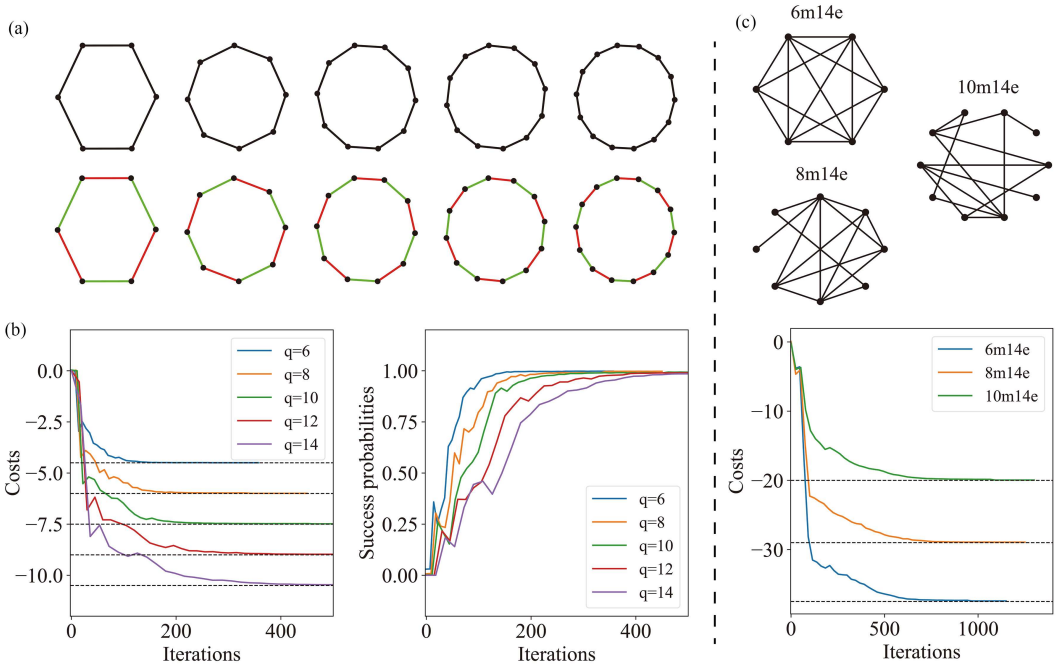

Figure 3 (Color online) (a) Testing Cycle graphs and their perfect matchings, where different colors represent different perfect matchings; (b) variational optimization process of the costs and success probabilities; (c) three sets of randomly generated test cases with 14 edges. 6m14e represents 6 nodes and 14 edges, and the rest are similar. The black dashed lines represent theoretical values.

Table 1 Test results of the Cycle graph under different qubit scales[a)]

	6 qubits	8 qubits	10 qubits	12 qubits	14 qubits
Params	24	32	40	48	56
Pm_ind	22, 41	86, 169	342, 681	1366, 2729	5462, 10921
Cost_theo	-4.500	-6.000	-7.500	-9.000	-10.500
Cost_sim	-4.495 ± 0.006	-5.986 ± 0.020	-7.486 ± 0.012	-8.984 ± 0.015	-10.472 ± 0.030
Suc_prob	0.998 ± 0.002	0.995 ± 0.008	0.995 ± 0.004	0.994 ± 0.005	0.989 ± 0.011

a) Params represents the number of parameters, Pm_ind represents the decimal index form of the perfect matching, Cost_theo represents the theoretical loss function value, Cost_sim is the loss function value under the optimal parameters for each optimization, Suc_prob is the success probability of sampling under the optimal parameters of each experiment, that is, the sum of the probabilities of all perfect matchings.

that the optimization process can be carried out very well. The success probabilities for the three groups of random graphs tested reached 0.946 ± 0.0431, 0.978 ± 0.003, and 0.953 ± 0.0489, respectively.

3.2 Effect of the variational depth

In order to study the influence of variational depth on the model, 1, 2, and 3 edges are added based on Cycle graph 6 to form experimental cases. Figure 4(a) shows the specific test graphs. The total qubits required are 7, 8, and 9. We select the circuit depth from 1 to 10. The decimal representations corresponding to the perfect matching sequence are $[38, 49, 73]$, $[26, 70, 97, 145]$, and $[52, 82, 140, 193, 266, 289]$. Figure 4(b) shows the change of costs and success probabilities with the number of iterations. We can see that with the increase in the number of iterations, the costs at different depths gradually decrease and converge, and the corresponding success probabilities almost increase and converge. Overall, the deeper the circuit, the more variational parameters are required, and the slower it converges. For a more detailed result, the cost and success probability of the optimal result for each of the five runs is shown in Table 2. We can see that the circuit achieves good results at shallow depths. Specifically, for the G_7, a circuit depth of 3 yields a success probability of 0.988 ± 0.006, for the G_8, a circuit depth of 3 yields a success probability of 0.956 ± 0.015, and for the G_9, a circuit depth of 2 yields a success probability 0.967 ± 0.020. Generally speaking, deeper circuits have more power in quantum computing. But when the capability of shallow circuits is sufficient to solve the problem, deeper circuits mean a waste of resources and redundancy. At the same time, due to the existence of quantum gate errors, the errors accumulated in deeper

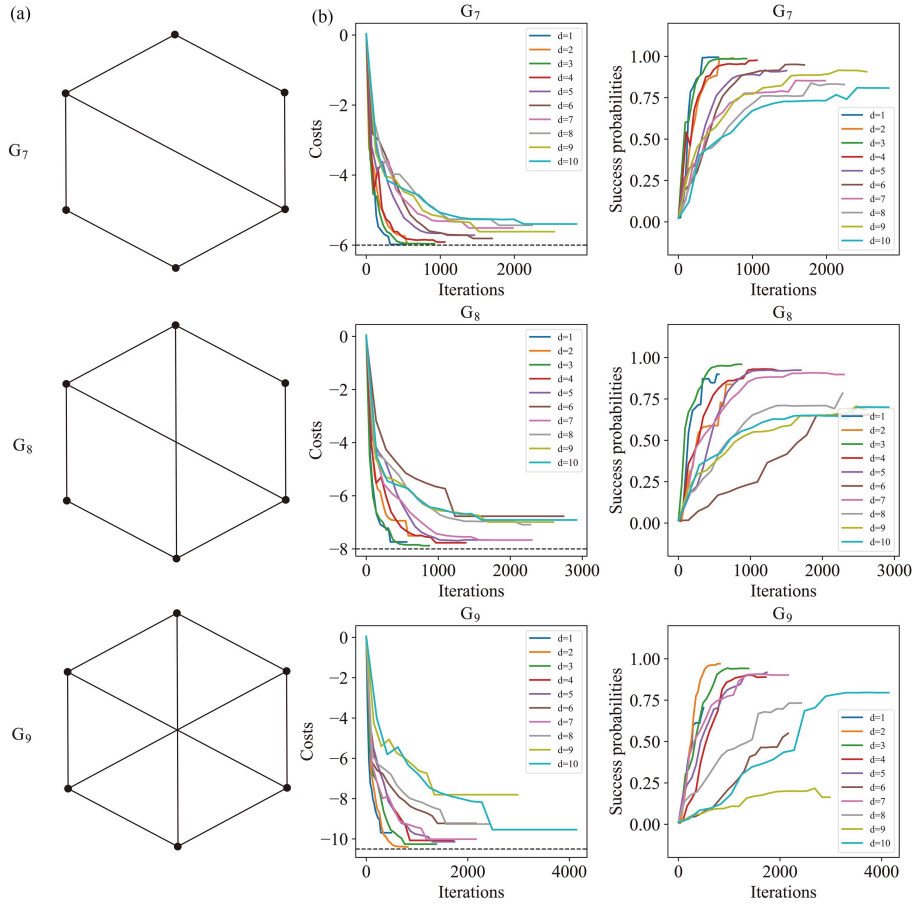

Figure 4 (Color online) (a) Different graphs used for testing. (b) Costs and success probabilities change during the variational optimization process of variational circuits with different depths, and the black dashed line represents the theoretical value.

Table 2 Test results of 7, 8, and 9 qubits under different variational depths[a)]

	7 qubits		8 qubits		9 qubits	
d	Suc_prob	Costs	Suc_prob	Costs	Suc_prob	Costs
1	0.893 ± 0.202	-5.770 ± 0.427	0.726 ± 0.355	-7.255 ± 1.051	0.500 ± 0.305	-9.188 ± 1.056
2	0.889 ± 0.195	-5.753 ± 0.419	0.600 ± 0.329	-6.982 ± 0.852	0.967 ± 0.020	-10.395 ± 0.067
3	0.988 ± 0.006	-5.966 ± 0.018	0.956 ± 0.015	-7.870 ± 0.052	0.942 ± 0.044	-10.282 ± 0.185
4	0.958 ± 0.020	-5.874 ± 0.064	0.885 ± 0.090	-7.608 ± 0.321	0.812 ± 0.226	-9.840 ± 0.831
5	0.898 ± 0.073	-5.695 ± 0.230	0.932 ± 0.028	-7.728 ± 0.128	0.862 ± 0.094	-9.966 ± 0.385
6	0.924 ± 0.050	-5.750 ± 0.148	0.427 ± 0.439	-6.229 ± 1.326	0.371 ± 0.269	-9.023 ± 0.600
7	0.797 ± 0.147	-5.387 ± 0.415	0.892 ± 0.048	-7.604 ± 0.192	0.805 ± 0.146	-9.606 ± 0.639
8	0.772 ± 0.159	-5.318 ± 0.401	0.715 ± 0.252	-7.030 ± 0.798	0.531 ± 0.215	-8.664 ± 0.869
9	0.841 ± 0.116	-5.437 ± 0.393	0.610 ± 0.160	-6.829 ± 0.496	0.173 ± 0.153	-7.278 ± 1.139
10	0.742 ± 0.205	-5.308 ± 0.512	0.637 ± 0.198	-6.757 ± 0.538	0.506 ± 0.305	-8.441 ± 1.234
Theory	–	-6.000	–	-8.000	–	-10.500

a) Theory represents the theoretical loss function value, Costs is the loss function value under the optimal parameters for each optimization, and Suc_prob is the success probability of sampling under the optimal parameters for each experiment.

circuits are more significant, thus reducing the probability of success. In the noisy intermediate scale quantum (NISQ) era, limited by the number of qubits, the fidelity of quantum gates, and the readout error, models with shallow circuit depths are often required to obtain better experimental results, and the proposed model can meet this well.

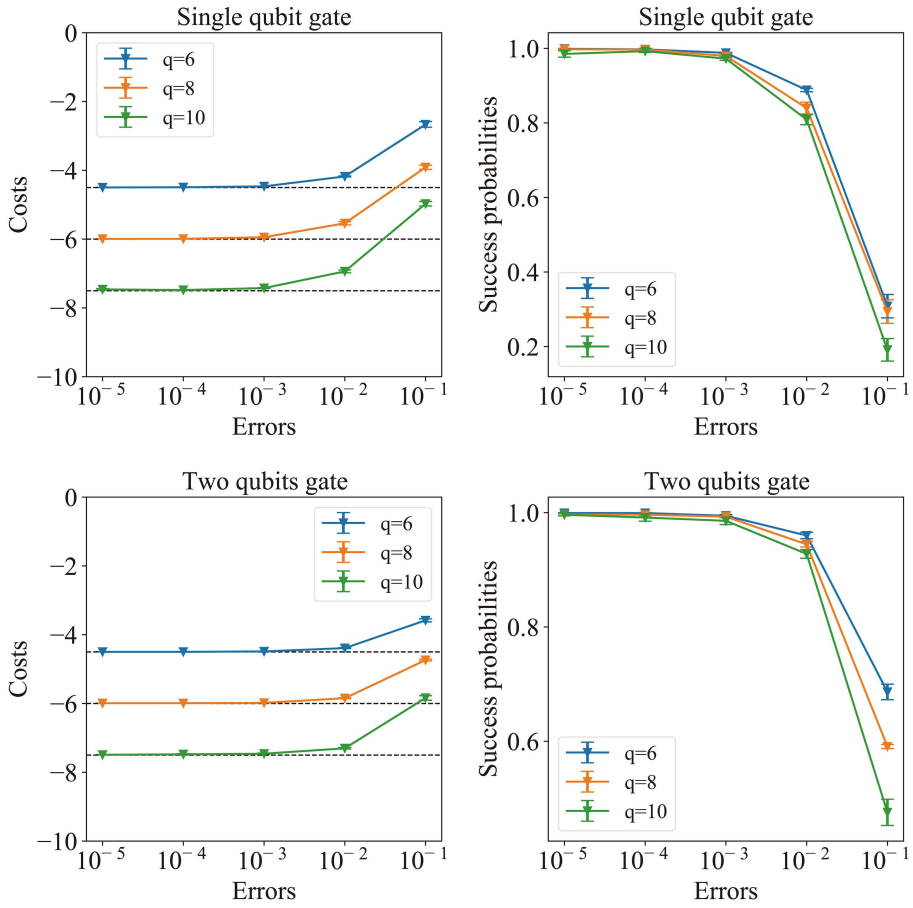

Figure 5 (Color online) Costs and success probabilities vary with single-qubit or two-qubit gates' dedepolarizing errors, with the black dashed line representing the theoretical value.

3.3 Effect of the noise

In general, quantum noise can be divided into depolarizing errors, Pauli errors, amplitude damping errors, phase damping errors, bit flipping errors, etc. [26]. The influence of depolarizing errors on the success probability of the model is considered here. For a quantum state ρ, depolarizing errors mean it has a probability p to be depolarized. That is, it has a probability p becoming a completely mixed state $I/2^n$, and a probability $1-p$ remaining the same. Mathematically it can be expressed as $\rho_{\text{end}} = (1-p)\rho + pI/(2^n)$, where error probability p is a freely adjusted parameter and n is the number of qubits. According to [27], when the circuit consists of two reversible randomly selected Clifford operators U and U^{-1}, where $UU^{-1} = I$, its average fidelity shows a linear growth trend with $(1-p)^m$, where m is the number of Clifford operators that make up U. However, the output quantum state of the proposed model is related to the graph of the input and cannot be predicted, so the influence of error on the success probability cannot be viewed from a global perspective and can only be studied with specific examples. Since the proposed model only has single qubit gates R_Y or R_Z and two-qubit gates CX, the following considers its influence on the success probability of the model. Here, the depolarizing errors encapsulated in Qiskit were used for simulation, with five replicates per optimization and 8196 samples per experiment. Take a cycle graph of 6, 8, and 10 qubits with layer $d = 1$ as an example, where the theoretical minimum energy value is $[-4.5, -6.0, -7.5]$. When the error of all single qubit gates and CX is set to $[0.1, 0.01, 0.001, 0.0001, 0.00001]$, respectively, the success probability of the model changes as in Figure 5, and it can be seen that the success probability increases as the error decreases. The larger the problem scale, the lower the success probability with the same error. For the test case, the depolarizing error of a single qubit gate has a greater effect than that of a two-qubit gate, mainly because the number of two-qubit gates increases by nearly 50% of that of a single qubit gate for each additional layer of the variational circuit. In addition, when the error of single-qubit or two-qubit gate is set to 0.001, the

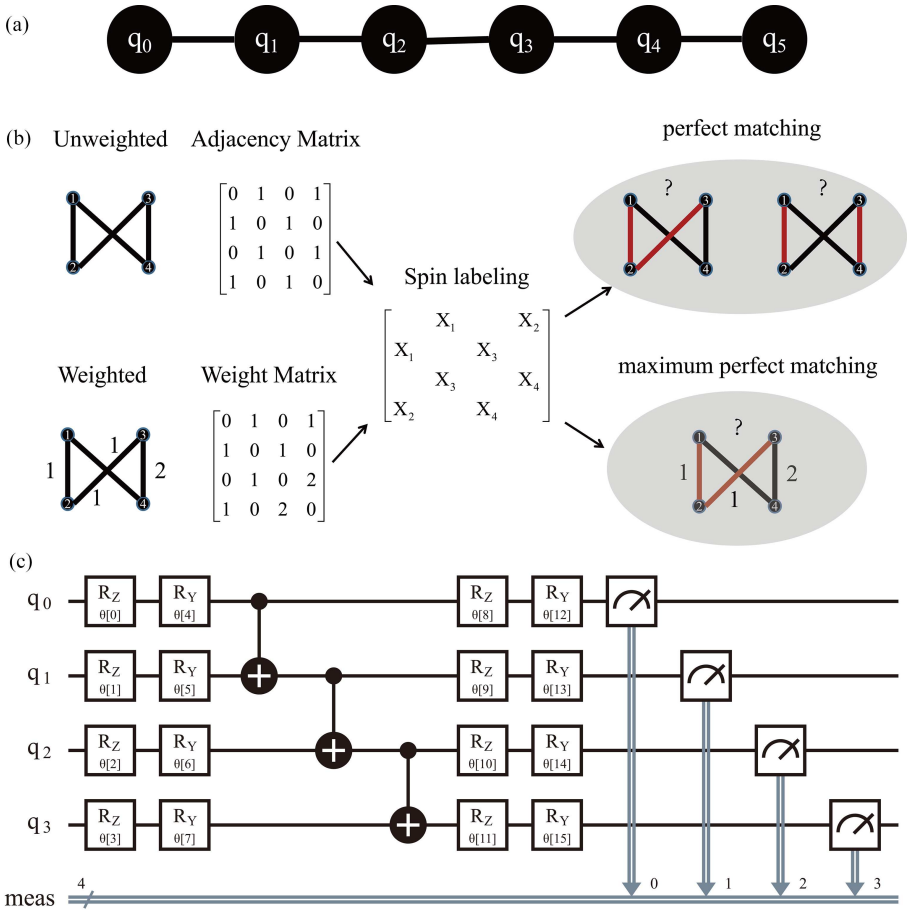

Figure 6 (Color online) (a) Topological structure diagram of "OriginQ Wuyuan" superconducting quantum computer; (b) four edges unweighted graph and weighted graph used in the experiment, and schematic diagram of the solution process; (c) experimental variational circuit diagram.

success probability of the model can reach more than 97%, respectively. This shows that the proposed model has good resistance to noise.

4 Experiments

The Origin Quantum Computing Technology Company is one of the leading quantum computing enterprises in China, and its official website has launched the quantum computing cloud platform. The platform provides the quantum simulation tool pyPanda and the 6-qubit superconducting quantum computer "OriginQ Wuyuan" [22] and provides a program interface for remote access [20]. The topology of "OriginQ Wuyuan" is shown in Figure 6(a). It shows that six qubits are connected in a chain and contain a set of logic gates that enable universal quantum computing. Table 3 shows more detailed prosperity of the superconducting quantum computer, including the operating frequency of each qubit, the $T1/T2$ time, the readout fidelity, the single-qubit gate fidelity, and the CZ gate fidelity. The experimental verification of the proposed model in this study is carried out on this quantum computer. Here, the unweighted graph and weighted graph of four edges are considered, and the graph to be solved and the solution process are shown in Figure 6(b). In order to solve this problem, a total of 4 qubits are required for the experiment. The single qubit variational operator is $R_Z(\theta 1)R_Y(\theta 2)$, the entanglement unit is four qubits linear entanglement, and the variational circuit depth is one layer. The circuit diagram used is shown in Figure 6(c), with a total of 16 parameters.

The experiment is divided into two parts: the first is to verify whether the quantum computer can correctly obtain all perfect matchings, and the second is whether the quantum computer can correctly obtain the maximum weighted perfect matching. The adjacency matrix of the graph is obtained first, then the edges are labeled according to the adjacency matrix, and each edge is mapped to a spin variable.

Table 3 Operating frequency, the $T1/T2$ time, the readout fidelity, the single-qubit gate fidelity, and the CZ gate fidelity of "OriginQ Wuyuan" superconducting quantum computer[a)]

Qubit	Frequency (MHz)	$T1/T2$ (μs)	Readout fidelity $F0/F1$	Single gate fidelity	CZ(i, j) fidelity
q0	5442	17/12.6	0.989/0.965	0.9993	(0,1)/0.9909
q1	4470	30/2.3	0.950/0.859	0.9990	(1,2)/0.9881
q2	5319	20/2.6	0.975/0.951	0.9990	(2,3)/0.9707
q3	4696	32/6.6	0.958/0.923	0.9991	(3,4)/0.9834
q4	5214.995	36/3.3	0.984/0.967	0.9992	(4,5)/0.9858
q5	4579.685	28/5.4	0.914/0.845	0.9992	–

a) The data in the table was archived from Origin Quantum Computing Technology's website [22] on April 23, 2023.

We use the COBYLA optimizer [24] to optimize the energy to obtain the minimum energy value, and count the costs and the success probability during each iteration (the success probability here is defined as the sum of the probabilities corresponding to the perfect matching in the sampling of the circuit under each set of parameter configuration). The answer is obtained based on the probability distribution corresponding to the lowest energy. Select the variational parameters corresponding to the lowest energy, sample the output distribution, and count the total probability corresponding to the perfect matching to obtain the final success probability. To explore whether the initialization of parameters affects the result, we consider two cases, the equal-weight superposition state, and the random state. For the equal weight superposition state, let all parameter values of the second column of the initialization operator be $\pi/2$, and all the remaining parameters be 0 so that the corresponding initial probability distribution is uniformly distributed, that is, the probability value of each item is 1/16. For random states, the value range of each parameter is limited to $(0, 2\pi)$. Each optimization was repeated five times with 1024 samples per test.

4.1 Perfect matching of the unweighted graph

For the unweighted graph in Figure 6(b), let $\alpha_1 = 1, \alpha_2 = 1, \alpha_3 = 0$. According to (11), the final Hamiltonian is

$$\begin{aligned} H &= H_1 + H_2 + H_3 \\ &= \{0.5 \times ZZII + 0.5 \times ZIZI + 0.5 \times IZIZ + 0.5 \times IIZZ + 2\}_{H_1} \\ &\quad + \left\{ \begin{array}{l} 0.5 \times ZZII + 0.5 \times ZIZI + 0.5 \times IZZI + 0.5 \times ZIIZ + 0.5 \times IZIZ \\ +0.5 \times IIZZ + 1 \end{array} \right\}_{H_2} \\ &= ZZII + ZIZI + 0.5 \times IZZI + 0.5 \times ZIIZ + IZIZ + IIZZ + 3. \end{aligned} \tag{14}$$

After obtaining the Hamiltonian, we conduct experiments according to Figure 1, ignore the constant term here, and test the optimization process from the equal weight superposition state and the random state initialization. Among them, costs represent energy, and success probabilities represent the sum of probabilities corresponding to perfect matchings. As can be seen from Figure 7(a), starting from the equal weight superposition state and the random state can eventually converge. As the optimization proceeds, the energy value gradually decreases and approaches the theoretical value -3, and the success probability gradually increases. Both can obtain the perfect matching with a high success probability, among which the equal weight simulation is 0.985 ± 0.017, the equal weight quantum is 0.803 ± 0.013, the random simulation is 0.990 ± 0.011, and the random quantum is 0.692 ± 0.079. Overall, the simulation results are better than the actual experiments. For quantum experiments, the final energy standard deviation of the equal-weight superposition state after convergence is significantly smaller than that of random initialization, which leads to a better success probability starting from the equal-weight superposition state than from the random state. In order to see what the final solution is, Figure 7(b) shows the mean value of the distribution D obtained under the optimal parameters in each optimization process. It can be seen that the probability is mainly concentrated in 6 (0110) and 9 (1001). The 4-digit binary expressions of 6 and 9 are 0110 and 1001, respectively. A bit of 0 in the binary expression indicates that the edge corresponding to the position is not selected, and a bit of 1 indicates that it is selected. Therefore, 0110 represents that the second edge (1, 4) and the third edge (2, 3) are selected, and 1001 represents that the first edge (1, 2) and the fourth edge (3, 4) are selected. These two sets $\{(1, 4), (2, 3)\}$ and $\{(1, 2), (3, 4)\}$ represent two perfect matchings of the test graph. For comparison, the bottom figure in Figure 7(b)

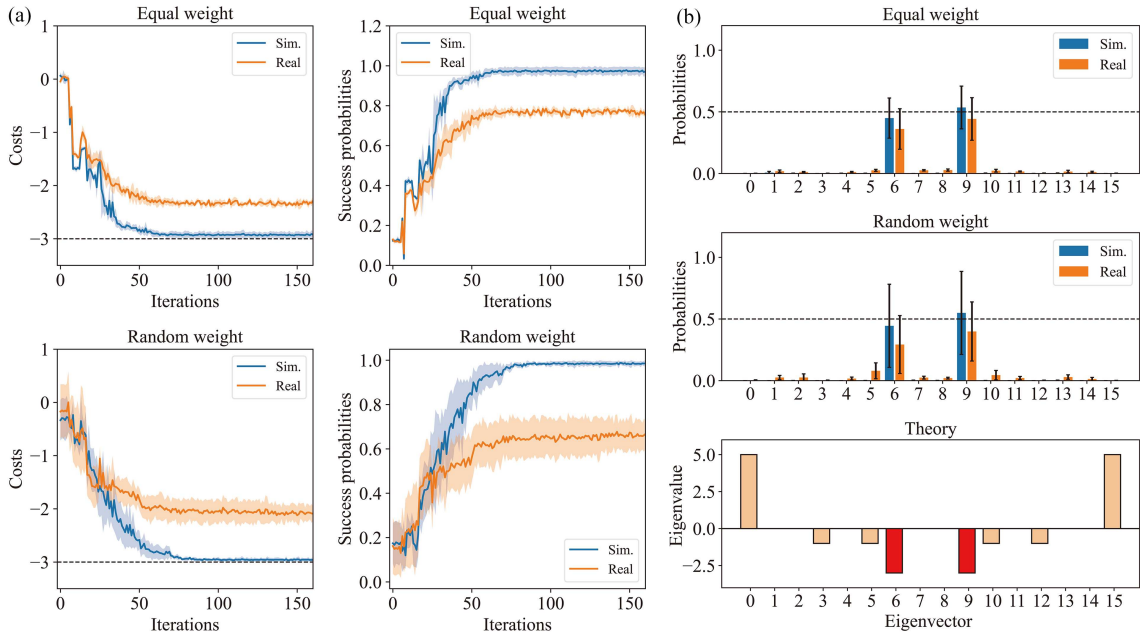

Figure 7 (Color online) Obtain all perfect matchings of the unweighted graph. (a) Costs and success probabilities change during the optimization process. The equal weight means that the initial states are equal-weight superposition states, and the random weight means that the initial states are random quantum states. Sim. is the simulation result, and Real is the test result on a real quantum computer. (b) The mean of the sampling distribution under the optimal parameters of multiple runs and the theoretical eigenvalue distribution of the Hamiltonian.

shows the distribution of eigenvalues after Hamiltonian decomposition. It can be seen that the minimum eigenvalue is -3, and its corresponding positions are 6 (0110) and 9 (1001), which are the two perfect matching indexes of the original graph. This shows that the model can achieve all perfect matchings, and the experiment is consistent with the theory.

4.2 Maximum weight perfect matching of the weighted graph

For the weighted graph in Figure 6(b), the weight of the fourth edge is 2, and the rest are 1. The goal at this time is to obtain the maximum weighted perfect matching of the graph. Let $\alpha_1 = 1, \alpha_2 = 1, \alpha_3 = -1$. According to (11), the final Hamiltonian is

$$\begin{aligned} H &= H_1 + H_2 + H_3 \\ &= \{0.5 \times ZZII + 0.5 \times ZIZI + 0.5 \times IZIZ + 0.5 \times IIZZ + 2\}_{H_1} \\ &\quad + \left\{ \begin{array}{l} 0.5 \times ZZII + 0.5 \times ZIZI + 0.5 \times IZZI + 0.5 \times ZIIZ + \\ 0.5 \times IZIZ + 0.5 \times IIZZ + 1 \end{array} \right\}_{H_2} \\ &\quad + \{ZIII + 0.5 \times IZII + 0.5 \times IIZI + 0.5 \times IIIZ - 2.5\}_{H_3} \\ &= ZIII + 0.5 \times IZII + 0.5 \times IIZI + 0.5 \times IIIZ + ZZII \\ &\quad + ZIZI + 0.5 \times IZZI + 0.5 \times ZIIZ + IZIZ + IIZZ + 0.5. \end{aligned} \tag{15}$$

We perform experiments according to Figure 1 after obtaining the Hamiltonian, where constant terms are ignored. The optimization processes initialized from the equal weight superposition state and the random state are tested in Figure 8(a), where costs represent energy and success probabilities represent the probabilities of the maximum weighted perfect matching. We can see that both the equal weight superposition state and the random state initialization can eventually converge. As the optimization processes, the energy value gradually decreases and approaches the theoretical value of -3.5, and the success probability gradually increases and converges. As shown in Figure 8(b), the correct answer can be obtained from both the equal weight superposition state and the random state initialization. Both can obtain the maximum weighted perfect matching with a high success probability, including the equal weight simulation with 0.974 ± 0.018, the equal weight quantum with 0.787 ± 0.020, the random

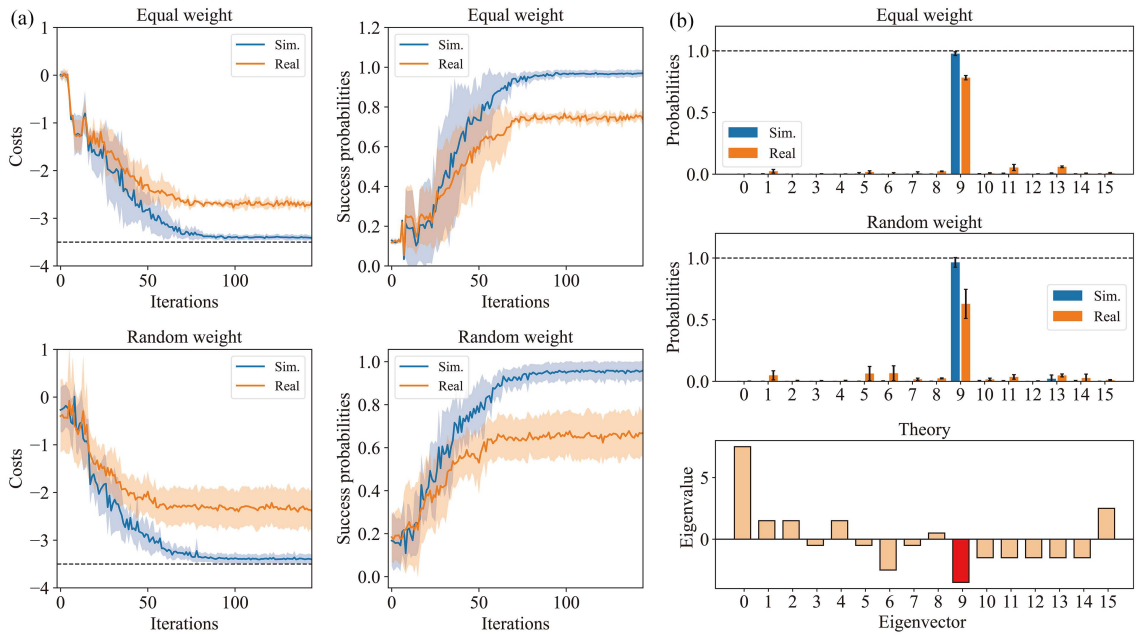

Figure 8 (Color online) Obtaining the maximum weight perfect matching of the weighted graph. (a) Changes in costs and success probabilities during the optimization process. The equal weight indicates that the initial state is an equal-weight superposition state, and the random weight indicates that the initial state is a random quantum state. Sim. is the simulation result, and Real is the test result on a real quantum computer. (b) The mean value of the sampling distribution under the optimal parameters of multiple runs and the theoretical eigenvalues distribution of the Hamiltonian.

simulation with 0.966 ± 0.039, and the random quantum with 0.610 ± 0.126. Overall, the results of the simulation are better than those of the quantum experiments. For quantum experiments, we gain a better success probability from the equal-weight superposition state than from the random state. In order to see what the final solution is, Figure 8(b) shows the mean of the resulting distribution D under the optimal parameters during each optimization. We can see that the probability is mainly concentrated on 9 (1001). For comparison, the bottom figure in Figure 8(b) shows the distribution of eigenvalues after Hamiltonian decomposition, and we can see that the minimum eigenvalue is -3.5, and its corresponding position is 9 (1001), which is the maximum weighted perfect matching index of the original graph. This shows that the experiment is consistent with the theory, and the model can correctly obtain the maximum weighted perfect matching.

5 Conclusion

In conclusion, in order to solve the problem of what exactly the perfect matchings of the graph are. We propose a QUBO formula for the perfect matchings and translate it into the Ising Hamiltonian. The Hamiltonian that ignores the constant term is the diagonal operator. By decomposing the Hamiltonian, we can obtain the solution to the problem according to the eigenvectors corresponding to the minimum eigenvalue. On one of Origin Quantum Computing Technology Company's quantum computers, we simulate and test the unweighted and weighted graphs of 4 edges. The experimental results show that for the setting of initial parameters for the variational quantum circuit, whether starting from the random state or from the equal weight superposition state, the loss function can eventually converge. After repeating the experiment multiple times, the success probability of perfect matchings or maximum weighted perfect matching can be significantly higher than that of other terms, and the test and simulation results match well. In terms of model scalability, we choose the Cycle graph for testing, and the scale of the simulation can support more than 14 qubits. In addition, we study the influence of noise on the proposed model and show that it can effectively resist the influence of depolarizing noise and obtain a high success probability at shallow variational depths. However, the proposed method also has some limitations. For example, as a hybrid model of a quantum annealing model and artificial intelligence (AI) method, the proposed method requires multiple samplings to obtain results and requires a combination of quantum and classical computers to run. In addition, due to the heuristic algorithm used in the optimization process, like other

AI methods, there is no guarantee that the best results will be obtained. However, this problem can be improved by increasing the number of repeated runs. The proposed model provides a new perspective for solving combinatorial optimization problems.

Acknowledgements This work was supported by National Key R&D Program of China (Grant No. 2019YFA0308700) and Innovation Program for Quantum Science and Technology (Grant No. 2021ZD0301500).

References

1 Krenn M, Gu X, Zeilinger A. Quantum experiments and graphs: multiparty states as coherent superpositions of perfect matchings. Phys Rev Lett, 2017, 119: 240403
2 Hall P. On representatives of subsets. J London Math Soc, 1935, s1-10: 26–30
3 Fenoaltea E M, Baybusinov I B, Zhao J Y, et al. The stable marriage problem: an interdisciplinary review from the physicist's perspective. Phys Rep, 2021, 917: 1–79
4 John P E. Kekulé count in toroidal hexagonal carbon cages. Croat Chem Acta, 1998, 71: 435–447
5 Salami M, Ahmadi M B. A mathematical programming model for computing the Fries number of a fullerene. Appl Math Model, 2015, 39: 5473–5479
6 Franco S, Hasan A. Graded quivers, generalized dimer models and toric geometry. J High Energy Phys, 2019, 2019: 104
7 Li D Y, Yan W G, Li S L. Solving combinatorially the monomer-dimer problem on certain fractal scale-free lattices. Adv Appl Math, 2022, 137: 102340
8 Hamilton C S, Kruse R, Sansoni L, et al. Gaussian boson sampling. Phys Rev Lett, 2017, 119: 170501
9 Arrazola J M, Bromley T R. Using Gaussian boson sampling to find dense subgraphs. Phys Rev Lett, 2018, 121: 030503
10 Huh J, Yung M H. Vibronic boson sampling: generalized Gaussian boson sampling for molecular vibronic spectra at finite temperature. Sci Rep, 2017, 7: 7462
11 Björklund A, Gupt B, Quesada N. A faster hafnian formula for complex matrices and its benchmarking on a supercomputer. ACM J Exp Algorithmics, 2019, 24: 1–17
12 Gupt B, Izaac J, Quesada N. The Walrus: a library for the calculation of hafnians, Hermite polynomials and Gaussian boson sampling. J Open Source Software, 2019, 4: 1705
13 Ryser H J. Combinatorial mathematics. Am Math Soc, 1963, 14: 24
14 Bokal D, Brešar B, Jerebic J. A generalization of Hungarian method and Hall's theorem with applications in wireless sensor networks. Discrete Appl Math, 2012, 160: 460–470
15 Brádler K, Dallaire-Demers P L, Rebentrost P, et al. Gaussian boson sampling for perfect matchings of arbitrary graphs. Phys Rev A, 2018, 98: 032310
16 Wan L X, Zhu H H, Wang B, et al. A boson sampling chip for graph perfect matching. In: Proceedings of CLEO: QELS Fundamental Science, 2022
17 Deng Y H, Gong S Q, Gu Y C, et al. Solving graph problems using Gaussian boson sampling. Phys Rev Lett, 2023, 130: 190601
18 Arrazola J M, Bromley T R, Rebentrost P. Quantum approximate optimization with Gaussian boson sampling. Phys Rev A, 2018, 98: 012322
19 Peruzzo A, McClean J, Shadbolt P, et al. A variational eigenvalue solver on a photonic quantum processor. Nat Commun, 2014, 5: 4213
20 Chen Z Y, Guo G P. QRunes: high-level language for quantum-classical hybrid programming. 2019. ArXiv:1901.08340
21 Wille R, Meter R V, Naveh Y. IBM's Qiskit tool chain: working with and developing for real quantum computers. In: Proceedings of Design, Automation & Test in Europe Conference & Exhibition (DATE), New York, 2019. 1234–1240
22 Zeng Y, Dong Z M, Wang H, et al. A general quantum minimum searching algorithm with high success rate and its implementation. Sci China Phys Mech Astron, 2023, 66: 240315
23 Lucas A. Ising formulations of many NP problems. Front Phys, 2014, 2: 5
24 Powell M J. A direct search optimization method that models the objective and constraint functions by linear interpolation. In: Proceedings of Advances in Optimization and Numerical Analysis, 1994. 51–67
25 Nannicini G. Performance of hybrid quantum-classical variational heuristics for combinatorial optimization. Phys Rev E, 2019, 99: 013304
26 Nielsen M A, Chuang I L. Quantum computation and quantum information. Phys Today, 2001, 54: 373–383
27 Alexander R N, Turner P S, Bartlett S D. Randomized benchmarking in measurement-based quantum computing. Phys Rev A, 2016, 94: 032303